Geophysical Research Letters

RESEARCH LETTER
10.1029/2021GL096709

Decadal Variability of Southeast US Rainfall in an Eddying Global Coupled Model

Wei Zhang[1,2,3], **Ben Kirtman**[4], **Leo Siqueira**[4], **Baoqiang Xiang**[2,5], **Johnna Infanti**[6], and **Natalie Perlin**[4]

[1]Program in Atmospheric and Oceanic Sciences, Princeton University, Princeton, NJ, USA, [2]NOAA/Geophysical Fluid Dynamics Laboratory, Princeton, NJ, USA, [3]NOAA/OAR/ESRL/Global Systems Laboratory, Boulder, Colorado, USA, [4]Rosenstiel School of Marine and Atmospheric Science, University of Miami, Miami, FL, USA, [5]Cooperative Programs for the Advancement of Earth System Science, University Corporation for Atmospheric Research, Boulder, CO, USA, [6]NOAA/NWS/NCEP/Climate Prediction Center, College Park, Innovim, LLC, Greenbelt, MD, USA

Key Points:

- Decadal rainfall pattern and associated mechanism in the Southeast US are examined from an eddying global coupled model
- Eddying CCSM4 improves the air-sea interactions in the Gulf Stream and the North Atlantic Subtropical High, modulating Southeast US rainfall
- Eddy-parameterizing CCSM4 and CMIP5 models may overestimate the role of tropical sea surface temperature in decadal Southeast US rainfall

Supporting Information:

Supporting Information may be found in the online version of this article.

Correspondence to:

W. Zhang,
wz19@princeton.edu

Citation:

Zhang, W., Kirtman, B., Siqueira, L., Xiang, B., Infanti, J., & Perlin, N. (2022). Decadal variability of Southeast US rainfall in an eddying global coupled model. *Geophysical Research Letters*, *49*, e2021GL096709. https://doi.org/10.1029/2021GL096709

Received 20 OCT 2021
Accepted 11 DEC 2021

Abstract

Ocean variability is a dominant source of remote rainfall predictability, but in many cases the physical mechanisms driving this predictability are not fully understood. This study examines how ocean mesoscales (i.e., the Gulf Stream SST front) affect decadal Southeast US (SEUS) rainfall, arguing that the local imprint of large-scale teleconnections is sensitive to resolved mesoscale features. Based on global coupled model experiments with eddying and eddy-parameterizing ocean, we find that a resolved Gulf Stream improves localized rainfall and remote circulation response in the SEUS. The eddying model generally improves the air-sea interactions in the Gulf Stream and the North Atlantic Subtropical High that modulate SEUS rainfall over decadal timescales. The eddy-parameterizing simulation fails to capture the sharp SST gradient associated with the Gulf Stream and overestimates the role of tropical Pacific SST anomalies in the SEUS rainfall.

Plain Language Summary

Current global climate models (GCMs) typically fail to fully resolve mesoscale ocean features (with length scales on the order of 10 km) such as western boundary currents, which potentially limit rainfall predictability over decadal timescales. Improvements in high-performance climate modeling enable us to incorporate high-resolution ocean models (0.1°) that capture these important mesoscale features with increased fidelity. Here we show that the inclusion of mesoscale ocean processes produces a more realistic Gulf Stream and improves both localized rainfall patterns and large-scale teleconnections. The high-resolution model shows a better representation of the air-sea interactions between the sea surface temperature and low-level atmosphere over the Gulf Stream, thus improving low-frequency rainfall variations over the Southeast US. The results further imply that high-resolution GCMs with increased ocean model resolution may be needed in future climate prediction systems.

1. Introduction

The ability to predict decadal rainfall variability over land remains one of the grand challenges in climate prediction. Regional prediction of rainfall has limited skill on timescales from seasons to decades (Hawkins & Sutton, 2011; Knutti & Sedláček, 2013; Kushnir et al., 2019; Pathak et al., 2019; Shepherd, 2014). For example, several recent studies have shown the underestimated signals in models, or the so-called "signal-to-noise paradox" (e.g., Scaife et al., 2014; Scaife & Smith, 2018; Siegert et al., 2016; Strommen & Palmer, 2019; Zhang et al., 2021; Zhang & Kirtman, 2019b) in decadal rainfall predictability (Smith et al., 2019), implying potentially serious issues in current modeling systems that fail to capture the observed decadal rainfall signals.

The ocean plays a crucial role in modulating low-frequency rainfall variability (see Battisti et al., 2019 for review of current understanding). Variations in sea surface temperature (SST) (e.g., El Niño/Southern Oscillation, ENSO) can result in substantial impacts on local air-sea feedbacks and teleconnection patterns affecting regional US precipitation variability (Grondona et al., 2000; Infanti & Kirtman, 2016; Mamalakis et al., 2018). However, extra-tropical mesoscale oceanic drivers of precipitation are not necessarily well represented in current GCMs (e.g., the fifth Coupled Model Intercomparison Project, CMIP5). In recent years, improvements in high-performance computing have enabled high-resolution GCMs with eddying (e.g., eddy-resolving and eddy-permitting) ocean models to include more mesoscale ocean processes (e.g., Delworth et al., 2012; Roberts et al., 2020; S. Wang et al., 2019; Zhang, 2020; Zhang et al., 2021). Studies with eddying GCMs show considerable benefits, for example, with better representation of ocean surface climatology (Kirtman et al., 2012; Siqueira & Kirtman, 2016), improvements in air-sea interactions (Bryan et al., 2010; Kirtman et al., 2017), and implications for remarkable impacts on precipitation changes especially over ocean regions (He et al., 2018).

Compared with their lower-resolution counterparts, eddying GCMs more accurately simulate fronts and the sharpness of SST gradients in the Gulf Stream (Siqueira & Kirtman, 2016) that are necessary to reproduce the observed distributions of the rainfall climatology (Bryan et al., 2010; Johnson et al., 2020; Minobe et al., 2008). Mesoscale air-sea interaction processes in the western boundary currents may influence the overlying atmospheric boundary layer and the upper troposphere and atmospheric circulation (Feliks et al., 2011; Siqueira et al., 2021; Small et al., 2008). Recent research by Zhang et al. (2021) performed coupled model experiments with eddy-resolving and eddy-parameterized ocean components and found better-represented subsurface ocean thermal and vertical structures along the Gulf Stream and its extension. The presence of ocean mesoscale features and associated vertical connectivity in eddy-resolving models contributes to increased decadal SST variability and predictability over the Gulf Stream and several other eddy-rich regions (Zhang et al., 2021). However, whether and the degree to which the inclusion of ocean mesoscales affects remote regional climate over land–particularly decadal Southeast US (SEUS) rainfall and teleconnections–remains unclear.

The motivation for addressing decadal SEUS rainfall variability in this study is twofold. Firstly, due to implications of increasing drought over the SEUS region in recent decades (e.g., Seager et al., 2009; H. Wang et al., 2010; Williams et al., 2017), understanding the variability of and mechanism for decadal-scale SEUS rainfall has considerable socioeconomic benefits in the management of agriculture, water supply, and ecosystem. This study is also motivated by recent findings in Infanti and Kirtman (2019), who ran a set of ensemble prediction experiments with and without a resolved ocean and argued that the resolved Gulf Stream could play a dominant role in the 36-month SEUS rainfall prediction. The mechanism for the increased prediction skills of multi-year SEUS rainfall with the eddy-resolving model is nevertheless unresolved.

Low-frequency SEUS rainfall significantly responds to ocean surface conditions and large-scale patterns of SSTs such as ENSO, the Pacific Decadal Oscillation (PDO) (e.g., Fuentes-Franco et al., 2016; L. Li et al., 2012), and the Atlantic Multi-decadal Oscillation (AMO) (e.g., Burgman & Jang, 2015; Kwon et al., 2009). For instance, ENSO can play an essential role in modulating seasonal to interannual SEUS rainfall variability, especially during winter seasons (Hoerling et al., 1997; Infanti & Kirtman, 2019; Schmidt et al., 2001; Trenberth et al., 1998). The impacts of tropical cyclones (Chan & Misra, 2010; Knight & Davis, 2007; Nogueira & Keim, 2011) and surface soil moisture (Yoon & Leung, 2015) on SEUS rainfall have also been addressed in previous studies. Of particular interest here is the North Atlantic subtropical high (NASH). W. Li et al. (2011) and W. Li et al. (2012) have noted that the displacement of the NASH western ridge influences the SEUS rainfall in summer by changing the moisture transport and vertical motion. The westward extension of the NASH toward the continental US contributes to increased northward flow and low-level convergence, leading to upward motion and more precipitation over the SEUS.

Here we diagnose how mesoscale ocean features affect decadal-scale SEUS precipitation and teleconnections based on the hypothesis that eddying model improves the simulations of the Gulf Stream SST and its connection with the NASH and hence regulates decadal SEUS rainfall variation. Possible influences of SSTs and the NASH on the SEUS rainfall at decadal timescales is discussed based on a suite of global coupled model simulations with the Community Climate System Model Version 4.0 (CCSM4; Gent et al., 2011) using eddying and eddy-parameterizing ocean component models.

2. Data and Method

2.1. Data

Observed monthly precipitation data are obtained from the Global Precipitation Climatology Project (GPCP) version 2.3 combined precipitation dataset (1979-present; Adler et al., 2018) and the gauge-based Global Precipitation Climatology Center (GPCC) precipitation product (1901–2016; Schneider et al., 2017) from the National Center for Atmospheric Research (NCAR). The GPCP data has a 40-year record and lower resolution on global 2.5° grids, whereas the GPCC provides land-surface precipitation with $1° \times 1°$ spatial resolution and a long-time record. To represent the NASH variability, we use the geopotential heights at 850 hPa from the NOAA's twentieth-century reanalysis version-2c data (20CV2c; Compo et al., 2011).

We assessed 30 coupled models from CMIP5 that were used as supplementary analyses (Table S1 in Supporting Information S1). All CMIP5 models are considered as low-resolution GCMs with an eddy-parametrized ocean. To equally weight each model, we only consider the first realization of each model's historical simulation. The results based on CMIP5 models are analyzed and compared with observational estimates.

2.2. Model Experiments

To examine the influence of ocean mesoscales on climate simulations, we perform two different sets of experiments using CCSM4 with eddy-parameterizing (1° ocean; hereafter, LRC) and eddying (0.1°; hereafter, HRC) ocean components, respectively. CCSM4 is a fully coupled climate model consisting of component models for atmosphere, land, ocean, sea ice, and the coupling infrastructure. A general description of CCSM4 can be found in Gent et al. (2011).

In this study, the LRC experiment is a present-day control simulation (greenhouse gas concentrations for 1990) using 1° atmosphere/land coupled to the ocean and sea-ice models with the nominal 1° horizontal resolution. LRC is initialized with an ocean at rest and allows for 200 years of spin-up period and then a 300-year simulation is integrated for analysis (the same simulation as used in Zhang & Kirtman, 2019a). HRC uses 0.5° atmosphere/land and nominal 1° horizontal resolution of the ocean and sea-ice component models. HRC experiments include three high-resolution simulations that are identical except for a small perturbation in the initial conditions. The initial condition for our first HRC simulation is taken from the end of the previously completed LRC experiment, and we ran the HRC model for 155 years and only analyzed the last 55 years. The two other HRC simulations are initialized, with small initial perturbations, at year 48 of the first, and run for 70 years. We drop the first 20-year of both of these simulations in our analysis. The details of CCSM4 HRC and LRC model experiments are discussed in Zhang et al. (2021). Thus, we have a total of 155 years of HRC and 300 years of LRC for analysis.

To diagnose the potential impact of atmospheric resolutions, we perform an additional experiment (hereafter, LRC-OCN) with a pre-released version of CCSM4, which has the same ocean and sea-ice model resolution (1°) as LRC and the exact atmospheric and land model resolution (0.5°) as HRC (see details in Kirtman et al., 2012). LRC-OCN has a present-day control simulation of 150 years, and the first 50 years are taken as spin-up periods.

3. Results and Discussion

We first show the observed (GPCC and GPCP) and model simulated (HRC and LRC) decadal variance of rainfall over the SEUS and western North Atlantic in Figure 1 (left panels). We removed any linear trend from the datasets and applied a 5-year low-pass Butterworth filter to the anomalies to represent internal rainfall variability at decadal timescales. Here we define the SEUS as land region bounded by 25° to 38° N and 266° to 284° E. Decadal SEUS rainfall variance is then estimated as the averaged variance of land grids within the dashed box in Figure 1a (with ocean grids masked). Compared with both observational estimates (GPCC: 0.12 mm^2/day^2; GPCP: 0.11 mm^2/day^2), the model simulations generally show smaller decadal SEUS rainfall variance. CMIP5 multi-model mean estimates (based on 30 model historical simulations in Table S1 in Supporting Information S1) show 21% lower decadal SEUS rainfall variance than observational estimates based on GPCP. Overall, CMIP5 models (73%), including CCSM4, underestimate decadal rainfall variance in the SEUS (Figure S1 in Supporting Information S1).

We identify an increase in the decadal variance of the SEUS rainfall in HRC (0.10 mm^2/day^2; Figure 1c) compared to LRC (0.08 mm^2/day^2; Figure 1d). Whether this improvement is due to finer ocean resolution remains unassessed in Figure 1 given that both the atmospheric and oceanic resolutions are different between LRC and HRC. However, the role of the ocean resolution is isolated in Figure S2 in Supporting Information S1. Here we note that the slightly larger decadal variance in SEUS rainfall detected in LRC-OCN (0.5° atmosphere; Figure S2a in Supporting Information S1) compared to LRC (1° atmosphere; Figure 1d) implies that the increased atmospheric resolution is also partially responsible for the increased variance, but the resolved ocean mesoscale features also remain important. We also note that even though the decadal SEUS rainfall variability is slightly larger in LRC-OCN (0.09 mm^2/day^2) compared to LRC, the rainfall climatology only indicates small differences (Figure S3 in Supporting Information S1). LRC, LRC-OCN, and HRC show similar Pearson's pattern correlations with observational estimates of decadal rainfall variance patterns, with coefficients ranging from 0.74 to 0.77. Pearson's pattern correlation analysis of the leading Empirical Orthogonal Function (EOF) patterns for decadal

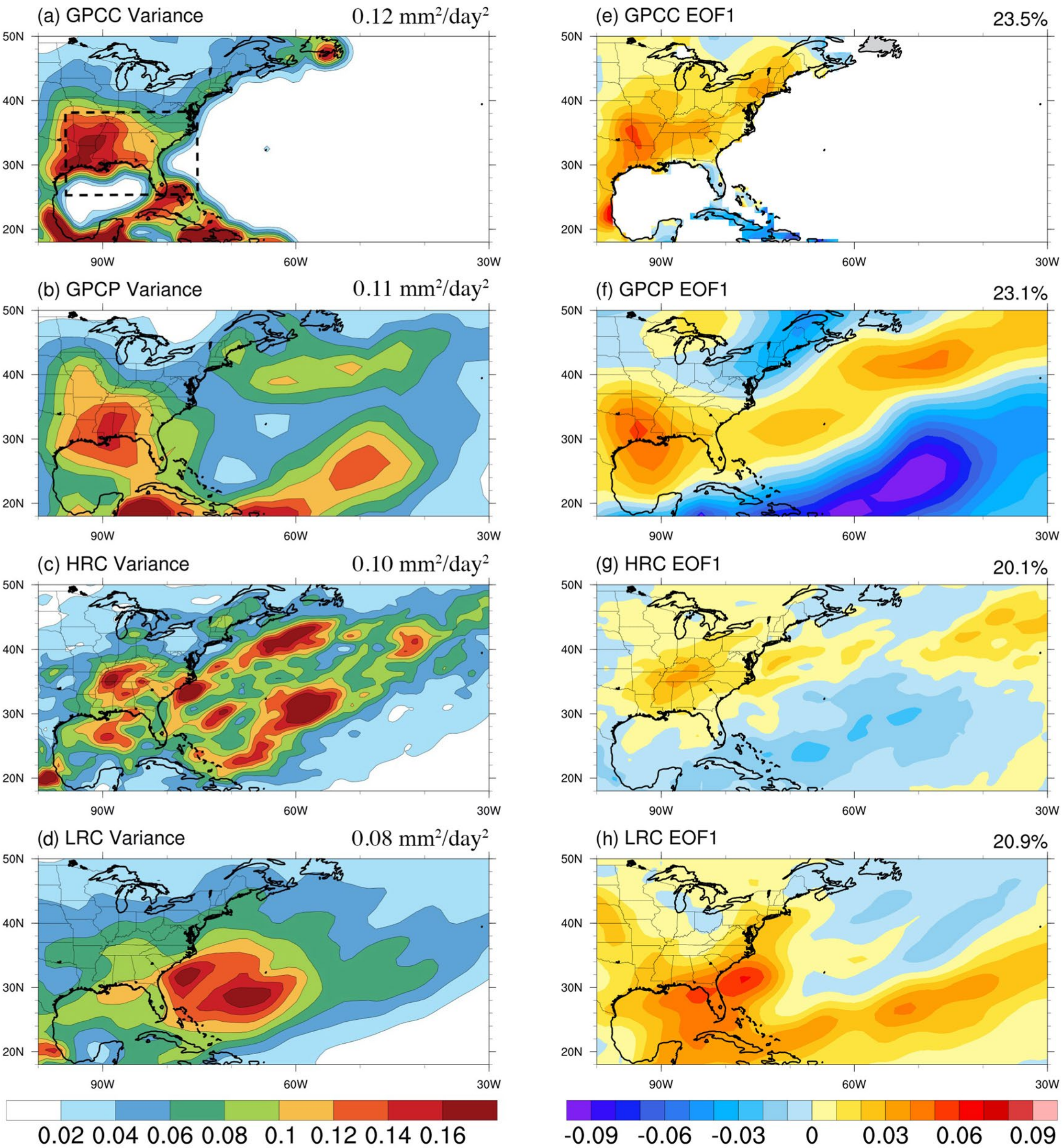

Figure 1. Decadal variance and leading EOF patterns (unit: mm/day) of monthly rainfall anomalies over the Southeast US and western North Atlantic region: (a), (e) GPCP, (b), (f) GPCP, (c), (g) LRC, and (d), (h) HRC. The land region within the black dashed box (25 to 38° N, 266° to 284° E; with ocean grids excluded) indicates the region of the Southeast US. Values of decadal SEUS rainfall variance for each observation and model simulation are shown on the top left corner of (a)–(d). All the data have been applied with a 5-year low-pass filter before analysis.

SEUS rainfall indicates that compared with LRC (0.28) and LRC-OCN (0.30), HRC is higher correlated with the observed EOF pattern with a coefficient of 0.42.

The leading EOF pattern of decadal rainfall variability in HRC (Figure 1g) suggests that a tilted zonal dipole over the ocean in HRC, similar to the GPCP observations (Figure 1f), is possibly linked to the Gulf Stream with maximum rainfall over the SEUS. However, the signal is weaker over SEUS than observational estimates (Figures 1e and 1f). The center of action in LRC and LRC-OCN (Figures 1h and S2b in Supporting Information S1) is further south and east of the observed and HRC. Although the increased atmospheric and land model resolution can play a role in decadal SEUS rainfall variability, HRC can generally capture the observed maximum rainfall signal over the SEUS in the leading EOF mode, which is missing in LRC and LRC-OCN. Besides, several earlier studies have identified better representation of the Gulf Stream SST climatology and decadal

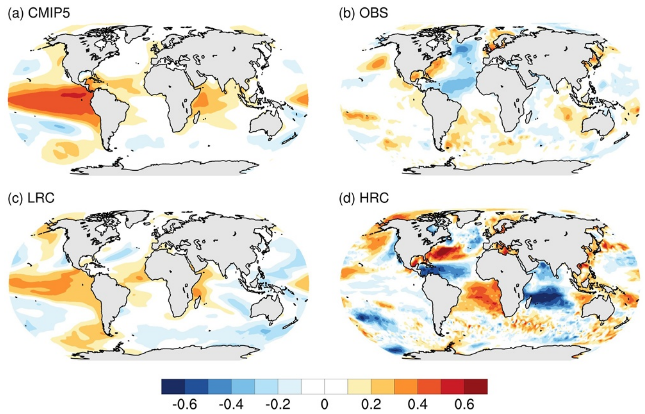

Figure 2. Correlation between decadal Southeast US rainfall index (25°–38°N, 266°–284°E) and global SST anomalies based on (a) CMIP5 (median correlation coefficients at each grid for 30 CMIP5 models), (b) OBS, (c) LRC, and (d) HRC. All the data have been applied with a 5-year low-pass filter. The maps only show the 95% confidence interval for the correlations based on the Student's *t* test (two-tailed).

variability with eddy-resolving CCSM4 compared with its lower-resolution counterparts that are eddy parameterized (Infanti & Kirtman, 2019; Siqueira & Kirtman, 2016; Zhang et al., 2021). Consistent with earlier research (e.g., Kirtman et al., 2012; Siqueira & Kirtman, 2016), we detect a warmer SST and sharper SST gradient especially along the Gulf Stream in HRC compared with LRC (Figure S4 in Supporting Information S1). Possible relationship between Gulf Stream SST and low-frequency SEUS rainfall in HRC instead of LRC has been reported by Infanti and Kirtman (2019) based on eddy-resolving CCSM4 initialized prediction experiments. Based on these differences we hypothesize that a more realistic Gulf Stream that resolved many mesoscale ocean processes is a partial contributor in decadal rainfall variability over the SEUS.

To examine the role of SST variability in modulating decadal SEUS rainfall, we show in Figure 2 the correlation between decadal SEUS rainfall index and global SST anomalies for the observational estimates and the models, with shading significant at 95% confidence level based on the Student's *t* test (two-tailed). The decadal SEUS rainfall index is defined as the area-averaged values of 5-year low-pass filtered rainfall anomalies over the SEUS (25°–38°N, 266°–284°E) land points. Both LRC and CMIP5 models (median correlation coefficients for 30 CMIP5 models) show a strong correlation between the decadal SEUS rainfall index and the tropical Pacific SST anomalies (Figures 2a and 2c). A similar pattern is also identified for LRC-OCN with finer atmospheric resolution than LRC (Figure S5 in Supporting Information S1). Compared with LRC, LRC-OCN shows even higher correlations between decadal SEUS rainfall and tropical Pacific SST anomalies (with coefficients up to 0.6), which indicates the potential impact of atmospheric internal variability on decadal SEUS rainfall (e.g., Seager et al., 2009). It is worth mentioning that the dominant role of tropical Pacific SST anomalies in decadal SEUS rainfall in LRC and CMIP5 models only occurs in winter seasons (Figure S6 in Supporting Information S1).

However, the strong positive link between the decadal SEUS rainfall index and topical SST signal is weak or even missing in HRC and observational estimates (Figures 2b and 2d). Interestingly, HRC and observational estimates suggests that decadal SST in the Gulf Stream and its surrounding regions can be the dominant contributor to decadal SEUS rainfall variability. We note that the correlation between decadal SEUS rainfall and Gulf Stream SST is detected in HRC is stronger than observational estimates, possibly because the spatial resolution of the currently available observed SST dataset–HadISST–is still too low to reproduce realistic decadal SST variability (Deser et al., 2010; Solomon & Newman, 2012), but we cannot eliminate the possibility that HRC overemphasizes the importance of the Gulf Stream variability. By estimating the pattern correlation of Figures 2a–2d against observational estimate (Figure 2b), we find that HRC shows higher pattern correlations (0.22; significant at 95% confidence level based on Pearson correlation) with observational estimates than LRC (0.02; insignificant) and CMIP5 model (−0.02; insignificant). A 0.22 correlation globally between HRC and observational estimates might still be low, but HRC does a better job in the region of interest, with a correlation of 0.55 in the North Atlantic. One possible interpretation of lower global but reasonable regional correlation is that model physics in HRC is happens to be tuned to represent the Gulf Stream and mesoscale ocean processes as best as it can in the North Atlantic, which may help reduce biases nearby. The authors are not aware of a specific tuning effort in this regard. Meanwhile, LRC shows strong pattern correlation with CMIP5, with a coefficient of 0.71 globally. We thus conclude that HRC produces an improvement of decadal SEUS rainfall induced teleconnections compared with LRC, indicating the significant impact of ocean mesoscales on the SEUS rainfall-SST teleconnections. We further argue that LRC and most CMIP5 models may overestimate the role of tropical Pacific SST in the SEUS rainfall over decadal timescales. This overestimation can be explained by the wintertime connection between SEUS rainfall and tropical Pacific SST anomalies. The results presented here are in good agreement with Infanti and Kirtman (2019), who argued that instead of tropical Pacific SST, the Gulf Stream played a leading role in the 36-month prediction of the SEUS precipitation (and drought). We also note that besides the Gulf Stream, decadal SST anomalies in the Indian Ocean and South Atlantic are strongly linked to decadal SEUS rainfall (Figure 2d). Compared with LRC, HRC indicates a significant increase of decadal SST variability over the Gulf Stream, South Atlantic and Indian Ocean (see figure 7 in Zhang et al., 2021). This enhanced decadal SST signal due to increased

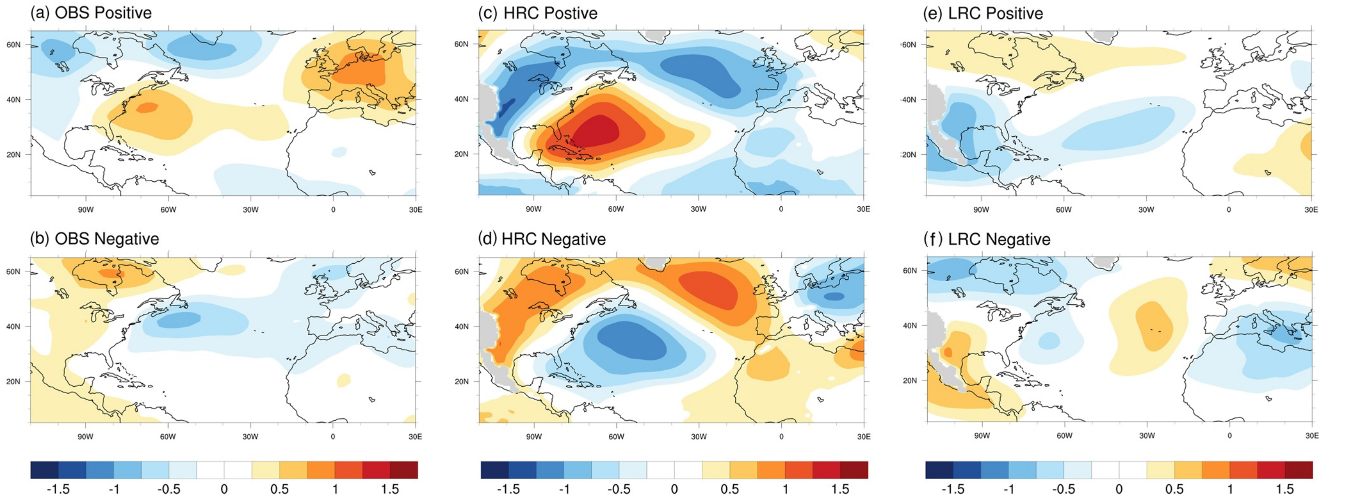

Figure 3. Composite of standardized decadal 850 hPa geopotential height anomalies (unit: m) during wet and dry conditions over the SEUS based on (a), (b) OBS, (c), (d) HRC, and (e), (f) LRC. Wet (dry) condition is identified when decadal SEUS rainfall index is above (below) plus (minus) one standard deviation.

ocean model resolution may influence remote regional climate such as low-frequency rainfall variability over the SEUS. SST signal on decadal timescales and longer is beyond the scope of the paper, and the focus is on the SEUS rainfall and SST anomalies in the Gulf Stream and its surroundings.

The influence of the NASH on interannual variations of the SEUS rainfall has been discussed in several earlier studies (e.g., W. Li et al., 2011; L. Li et al., 2012). Here we aim to investigate the role of the NASH in decadal SEUS rainfall variability by comparing HRC with LRC. We focus on 850 hPa geopotential heights as it is a common indicator for the NASH. Figure 3 shows the composite of standardized decadal 850 hPa geopotential height anomalies during wet and dry conditions over the SEUS. The corresponding composite of standardized decadal SST anomalies during wet and dry conditions is also shown in Figure S7 in Supporting Information S1. During the SEUS wet conditions, the warm SST and strong high-pressure anomalies along the Gulf of Mexico, SEUS, and Gulf Stream in HRC produce increased northward moisture transport and low-level convergence (as shown in Figure S8a in Supporting Information S1), which leads to upward motion and ultimately more precipitation over the SEUS. We argue this increased rainfall is due to the westward extension of the NASH (Jones, 2019; W. Li et al., 2011; L. Li et al., 2012). During the SEUS dry conditions, we find cold SST anomalies along the Gulf Stream and a robust low-pressure anomaly centered around the Gulf Stream extension in HRC, contributing to southward flow and low-level divergence (Figure S8b in Supporting Information S1) and thus downward motion and less precipitation over the SEUS. As suggested by W. Li et al. (2011) and L. Li et al. (2012), the westward extension and retreat of the NASH plays a leading role in modulating summer rainfall variability over the SEUS. While the results shown here focus on low-frequency filtered data, the summer season dominates since this is when the SEUS rainfall is maximum. Observational seasonality analysis (Figure S9 in Supporting Information S1) demonstrates that compared with winter season (climatology: 3.27 mm/day; standard deviation: 0.19 mm/day), summer SEUS rainfall variability (climatology: 4.23 mm/day; standard deviation: 0.23 mm/day) makes up a relatively larger component of annual mean precipitation. The results presented generally capture the southwest pattern of the NASH western ridge (see Figure 3 in L. Li et al., 2012), implying that the westward movement of NASH regulates decadal-scale rainfall variability over the SEUS region. HRC generally resembles the spatial patterns of the NASH variability based on observational estimates, though HRC somewhat overestimates the amplitude of the decadal NASH pressure anomalies and its connection to the SEUS rainfall (Figure 3). To quantify how well HRC captures the observed NASH-SEUS rainfall relationship in Figure 3, we estimate the pattern correlation of Figures 3c and 3e against Figure 3a. The results show that HRC (0.51) is better correlated with the observational estimates than LRC (−0.34). Similar results are found when computing the pattern correlation of Figures 3d and 3e against Figure 3f. Although HRC may overestimate the role of the NASH in the SEUS rainfall, HRC better reproduces the NASH-SEUS rainfall relationship (Figure 4) compared to LRC.

LRC, conversely, fails to capture decadal NASH variability and its connection to the SEUS rainfall. For example, LRC largely fails to capture the westward expansion or shift of the NASH that is apparent in the observational

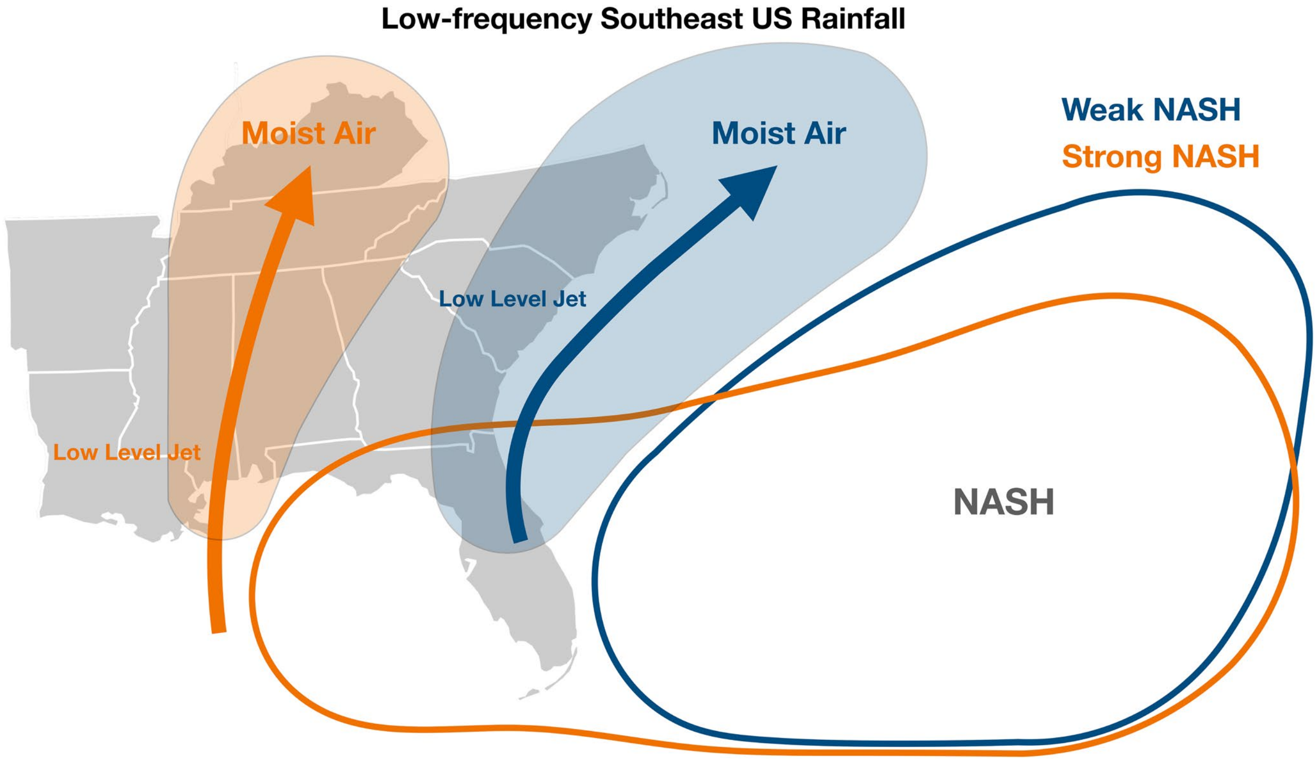

Figure 4. Diagram of the westward extension of the NASH for increased rainfall over the Southeast US.

estimates and in HRC. Changes in decadal SEUS rainfall in LRC are possibly due to variations of the pressure anomaly centers over the western US (Figures 3e and 3f) and eastern tropical Pacific. LRC shows much weaker decadal SST-NASH correlations especially over the Gulf Stream (and mid-latitude North Atlantic) than HRC, implying different roles of the Gulf Stream SST in decadal NASH variability with and without a resolved Gulf Stream (Figure S10 in Supporting Information S1). The strong link between the Gulf Stream SST and the NASH is further supported by Figure S10 in Supporting Information S1, showing that the low-frequency filtered Gulf Stream SST index in HRC is strongly correlated with the NASH over the Gulf Stream and tropical North Atlantic. A warmer SST around the Gulf Stream in HRC than LRC (Figure S4 in Supporting Information S1) vary coherently with a higher low-level geopotential height (Figure S11 in Supporting Information S1), which is related to a wet condition (more precipitation) over the SEUS (Figure 3). Compared with HRC, the Gulf Stream SST-NASH correlation is weaker in LRC (Figure S11b in Supporting Information S1). The pattern in HRC (Figure S11a in Supporting Information S1) generally mimics the pattern between SEUS rainfall and the NASH as shown in Figures 3c and 3d, indicating the close relationships among the Gulf Stream SST, NASH and SEUS rainfall variability.

It is noted that there is a strong positive correlation between the SST and 850 hPa geopotential height anomalies around the Gulf Stream (Figure 3 and S7 and S11 in Supporting Information S1), which is inconsistent with the results of several earlier research showing the negative correlation between the mid-latitude SST and pressure in the lower troposphere (e.g., Fink et al., 2012; Minobe et al., 2008; Sugimoto et al., 2021; Xu et al., 2010). As shown by Minobe et al. (2008), for example, mesoscale warm (cold) SST decreases (increases) the surface pressure over the Gulf Stream. One possible interpretation for the positive correlation between the SST and low-level geopotential height (pressure) anomalies is the atmospheric influence on the SST. In HRC and observations, high (low) pressure anomalies contribute to a decrease (an increase) in cloud cover, increasing (decreasing) solar radiation and warming (cooling) the SST under the high (low) pressure anomalies.

Moreover, the resolved Gulf Stream also shows strong correlations with decadal SST variability over the Southern Atlantic (positive), Indian Ocean (negative), and Kuroshio Current (positive) in HRC (Figure S12 in Supporting Information S1). The correlations shown in Figure 2 and S11 and S12 in Supporting Information S1 support the argument that the NASH, SEUS rainfall and the Gulf Stream SST vary coherently on decadal timescale and that much of this coherence in the observational estimates and HRC is missing in LRC and the CMIP models. We note that in HRC, the Gulf Stream SST and global SSTA have relatively large correlations in regions that are quite remote from the North Atlantic, and we cannot rule out that these remote SSTA can affect the NASH and the SEUS rainfall. Relatively large correlations cannot be used to detect causal relationship–addition numerical experiments are required, although this is beyond the current study. Nevertheless, we can conclude that the relationship between NASH, SEUS rainfall, and the Gulf Stream SST is markedly different in the observational estimates and HRC compared to LRC and the CMIP models, and we assert that this is largely due to resolved ocean mesoscale processes.

4. Summary and Conclusion

This study investigates decadal SEUS rainfall and its teleconnections using high-resolution eddying CCSM4 simulations compared with its lower-resolution counterparts that are eddy parameterized. With better resolved mesoscale processes, the simulations indicate an improved annual mean rainfall climatology along the Gulf Stream that is generally consistent with observational estimates. We find no notable improvement in the annual mean rainfall climatology over the SEUS, whereas enhanced decadal SEUS rainfall variance is detected with HRC in better agreement with observational estimates. Though atmospheric resolution may partly contribute to the increase in the decadal variance of the SEUS rainfall, the leading EOF pattern in HRC shows consistency with observations, indicating the influence of the resolved Gulf Stream with a local maximum over the SEUS. This dominant rainfall pattern in HRC and observational estimates is not the leading pattern in LRC or LRC-OCN, and thus, we conclude that this decadal variability is connected to resolved Gulf Stream variability.

The above conclusion is further supported by the decadal SEUS rainfall teleconnections with global SST. Consistent with Infanti and Kirtman (2019), the SEUS rainfall shows a higher correlation with the North Atlantic SST than the tropical Pacific SST on decadal timescales in HRC and observations. HRC suggests an even higher correlation between decadal SEUS rainfall and the Gulf Stream SST than observational estimates, perhaps indicating that HRC over-predicts the connectivity between Gulf Stream variability and decadal SEUS rainfall variability. Conversely, LRC and CMIP5 models overestimate the role of tropical Pacific SST anomalies in decadal SEUS rainfall. Although the seasonality of decadal SEUS rainfall is not our focus in this manuscript, we re-examine the SEUS rainfall-SST relationship in the summer and winter seasons, respectively. Perhaps surprising is that the overall correlation patterns, as shown in Figure 2, pick up the wintertime relationships (Figure S6 in Supporting Information S1). Interestingly, HRC and observation show a positive (negative) correlation between the SEUS rainfall and tropical Pacific SST during winter (summer). Decadal SEUS rainfall shows no discernable connection with tropical Pacific SST because the summer and winter anomalies cancel each other.

A resolved Gulf Stream (SST) suggests a strong link with the NASH variations. Different from previous studies (Minobe et al., 2008; Sugimoto et al., 2021; Xu et al., 2010), we detect a positive correlation between the SST and the NASH anomalies over the mid-latitude western North Atlantic, implying the atmospheric influence on the SST along the Gulf Stream. An eddying coupled model improves the representation of air-sea interaction and the NASH variations, regulating decadal SEUS rainfall variability. HRC can generally reproduce the observed westward extension and retreat of the NASH that regulates the variations of decadal SEUS rainfall (Figures 3 and 4), despite that HRC may overestimate the correlation between the SEUS rainfall and NASH. As suggested in HRC and observations, the westward extension of the NASH brings increased northward moisture transport and low-level convergence, leading to rising motion and ultimately more rainfall in the SEUS, which can be explained by a steady-state quasi-geostrophic balance. However, the LRC simulation fails to capture the realistic Gulf Stream, the westward extension of the NASH, and its relationship with the SEUS rainfall.

Uncertainty remains in this study as the length of high-resolution observation and model simulations is limited, and the results may be model-dependent. We acknowledge that there are possible caveats to our results and proposed dynamics. We argue that an eddying coupled model improves the air-sea interactions in the Gulf Stream and the North Atlantic Subtropical High, modulating SEUS rainfall variability. It remains debatable whether the ocean or the atmosphere plays a more significant role in the air-sea interaction and associated SEUS rainfall with more mesoscale ocean processes included. Besides, many other factors that may influence decadal SEUS rainfall such as tropical cyclone activities and surface soil moisture are not addressed. However, this study, for the first time, demonstrates the potential benefits of an ocean eddying GCMs for regional rainfall simulations and predictions over land. Arguably, the results presented here demonstrate that using models that capture oceanic mesoscale features have the potential to improve the representation of rainfall variability remotely and regionally. How well this translates across models remains an open question and whether this improved simulated low-frequency variability of remote rainfall translates into improved predictions remains an open question.

Data Availability Statement

All the observational, reanalysis data and CMIP5 historical simulations are properly referenced and publicly available. The GPCP and GPCC precipitation datasets are downloaded through https://psl.noaa.gov/data/gridded/data.gpcp.html and https://psl.noaa.gov/data/gridded/data.gpcc.html, respectively. The twentieth century reanalysis of geopotential height at 850 hPa can be found from NOAA's Physical Sciences Laboratory (https://psl.noaa.gov/data/20thC_Rean). Thirty CMIP5 model historical simulations and the associated model descriptions can be obtained from https://esgf-node.llnl.gov/search/cmip5. The CMIP5 models used in the study are listed in Table S1 in Supporting Information S1. The Southeast US rainfall index (5-year low-pass filtered) derived from observations and models can be accessed by using the DOI http://doi.org/10.5281/zenodo.4433147. Besides, the model codes of CCSM4 can be accessed from http://www.cesm.ucar.edu/models/ccsm4.0/. The CCSM4 HRC and LRC model simulations used in this study have been archived at https://doi.org/10.5281/zenodo.5057616.

Acknowledgments
This report is prepared by Wei Zhang under award NA18OAR4320123 from the National Oceanic and Atmospheric Administration, U.S. Department of Commerce. The statements, findings, conclusions, and recommendations are those of the author(s) and do not necessarily reflect the views of the National Oceanic and Atmospheric Administration, or the U.S. Department of Commerce. Ben Kirtman and Leo Siqueira acknowledge the support from NOAA (NA18OAR4310293, NA15OAR4320064), NSF (OCE1419569, OCE1559151), and DOE (DE-SC0019433). We thank Nathaniel C. Johnson and Yongqiang Sun from NOAA GFDL for providing internal review.

References

Adler, R. F., Sapiano, M. R., Huffman, G. J., Wang, J. J., Gu, G., Bolvin, D., et al. (2018). The Global Precipitation Climatology Project (GPCP) monthly analysis (new version 2.3) and a review of 2017 global precipitation. *Atmosphere*, *9*(4), 138. https://doi.org/10.3390/atmos9040138

Battisti, D. S., Vimont, D. J., & Kirtman, B. P. (2019). 100 Years of progress in understanding the dynamics of coupled atmosphere–ocean variability. *Meteorological Monographs*, *59*, 8–1. https://doi.org/10.1175/AMSMONOGRAPHS-D-18-0025.1

Bryan, F. O., Tomas, R., Dennis, J. M., Chelton, D. B., Loeb, N. G., & McClean, J. L. (2010). Frontal scale air–sea interaction in high-resolution coupled climate models. *Journal of Climate*, *23*(23), 6277–6291. https://doi.org/10.1175/2010JCLI3665.1

Burgman, R. J., & Jang, Y. (2015). Simulated US drought response to interannual and decadal Pacific SST variability. *Journal of Climate*, *28*(12), 4688–4705. https://doi.org/10.1175/JCLI-D-14-00247.1

Chan, S. C., & Misra, V. (2010). A diagnosis of the 1979–2005 extreme rainfall events in the southeastern United States with isentropic moisture tracing. *Monthly Weather Review*, *138*(4), 1172–1185. https://doi.org/10.1175/2009MWR3083.1

Compo, G. P., Whitaker, J. S., Sardeshmukh, P. D., Matsui, N., Allan, R. J., Yin, X., et al. (2011). The twentieth century reanalysis project. *Quarterly Journal of the Royal Meteorological Society*, *137*(654), 1–28. https://doi.org/10.1002/qj.776

Delworth, T. L., Rosati, A., Anderson, W., Adcroft, A. J., Balaji, V., Benson, R., et al. (2012). Simulated climate and climate change in the GFDL CM2. 5 high-resolution coupled climate model. *Journal of Climate*, *25*(8), 2755–2781. https://doi.org/10.1175/JCLI-D-11-00316.1

Deser, C., Phillips, A. S., & Alexander, M. A. (2010). Twentieth century tropical sea surface temperature trends revisited. *Geophysical Research Letters*, *37*(10). https://doi.org/10.1029/2010GL043321

Feliks, Y., Ghil, M., & Robertson, A. W. (2011). The atmospheric circulation over the North Atlantic as induced by the SST field. *Journal of Climate*, *24*(2), 522–542. https://doi.org/10.1175/2010JCLI3859.1

Fink, A. H., Pohle, S., Pinto, J. G., & Knippertz, P. (2012). Diagnosing the influence of diabatic processes on the explosive deepening of extratropical cyclones. *Geophysical Research Letters*, *39*(7). https://doi.org/10.1029/2012GL051025

Fuentes-Franco, R., Giorgi, F., Coppola, E., & Kucharski, F. (2016). The role of ENSO and PDO in variability of winter precipitation over North America from twenty first century CMIP5 projections. *Climate Dynamics*, *46*(9–10), 3259–3277. https://doi.org/10.1007/s00382-015-2767-y

Gent, P. R., Danabasoglu, G., Donner, L. J., Holland, M. M., Hunke, M., Jayne, C., et al. (2011). The community climate system model version 4. *Journal of climate*, *24*(19), 4973-4991. https://doi.org/10.1175/2011JCLI4083.1

Grondona, M. O., Podestá, G. P., Bidegain, M., Marino, M., & Hordij, H. (2000). A stochastic precipitation generator conditioned on ENSO phase: A case study in southeastern south America. *Journal of Climate*, *13*(16), 2973–32986. https://doi.org/10.1175/1520-0442(2000)013<2973:ASPGCO>2.0

Hawkins, E., & Sutton, R. (2011). The potential to narrow uncertainty in projections of regional precipitation change. *Climate Dynamics*, *37*(1–2), 407–418. https://doi.org/10.1007/s00382-010-0810-6

He, J., Kirtman, B., Soden, B. J., Vecchi, G. A., Zhang, H., & Winton, M. (2018). Impact of ocean eddy resolution on the sensitivity of precipitation to CO_2 increase. *Geophysical Research Letters*, *45*(14), 7194–7203. https://doi.org/10.1029/2018GL078235

Hoerling, M. P., Kumar, A., & Zhong, M. (1997). El Niño, La Niña, and the nonlinearity of their teleconnections. *Journal of Climate*, *10*(8), 1769–21786. https://doi.org/10.1175/1520-0442(1997)010<1769:ENOLNA>2.0.CO;2

Infanti, J. M., & Kirtman, B. P. (2016). North American rainfall and temperature prediction response to the diversity of ENSO. *Climate Dynamics*, *46*(9–10), 3007–3023. https://doi.org/10.1007/s00382-015-2749-0

Infanti, J. M., & Kirtman, B. P. (2019). A comparison of CCSM4 high-resolution and low-resolution predictions for south Florida and southeast United States drought. *Climate Dynamics*, *52*(11), 6877–6892. https://doi.org/10.1007/s00382-018-4553-0

Johnson, N. C., Krishnamurthy, L., Wittenberg, A. T., Xiang, B., Vecchi, G. A., Kapnick, S. B., & Pascale, S. (2020). The impact of sea surface temperature biases on North American precipitation in a high-resolution climate model. *Journal of Climate*, *33*(6), 2427–2447. https://doi.org/10.1175/JCLI-D-19-0417.1

Jones, C. (2019). Recent changes in the South America low-level jet. *npj Climate and Atmospheric Science*, *2*(1), 1–8. https://doi.org/10.1038/s41612-019-0077-5

Kirtman, B. P., Bitz, C., Bryan, F., Collins, W., Dennis, J., Hearn, N., et al. (2012). Impact of ocean model resolution on CCSM climate simulations. *Climate Dynamics*, *39*(6), 1303–1328. https://doi.org/10.1007/s00382-012-1500-3

Kirtman, B. P., Perlin, N., & Siqueira, L. (2017). Ocean eddies and climate predictability. *Chaos: An Interdisciplinary Journal of Nonlinear Science*, *27*(12), 126902. https://doi.org/10.1063/1.4990034

Knight, D. B., & Davis, R. E. (2007). Climatology of tropical cyclone rainfall in the southeastern United States. *Physical Geography*, *28*(2), 126–147. https://doi.org/10.2747/0272-3646.28.2.126

Knutti, R., & Sedláček, J. (2013). Robustness and uncertainties in the new CMIP5 climate model projections. *Nature Climate Change*, *3*(4), 369–373. https://doi.org/10.1038/nclimate1716

Kushnir, Y., Scaife, A. A., Arritt, R., Balsamo, G., Boer, G., Doblas-Reyes, F., et al. (2019). Towards operational predictions of the near-term climate. *Nature Climate Change*, *9*(2), 94–101. https://doi.org/10.1038/s41558-018-0359-7

Kwon, H. H., Lall, U., & Obeysekera, J. (2009). Simulation of daily rainfall scenarios with interannual and multidecadal climate cycles for South Florida. *Stochastic Environmental Research and Risk Assessment*, *23*(7), 879–896. https://doi.org/10.1007/s00477-008-0270-2

Li, L., Li, W., & Kushnir, Y. (2012). Variation of the North Atlantic subtropical high western ridge and its implication to Southeastern US summer precipitation. *Climate Dynamics*, *39*(6), 1401–1412. https://doi.org/10.1007/s00382-011-1214-y

Li, W., Li, L., Fu, R., Deng, Y., & Wang, H. (2011). Changes to the North Atlantic subtropical high and its role in the intensification of summer rainfall variability in the southeastern United States. *Journal of Climate*, *24*(5), 1499–1506. https://doi.org/10.1175/2010JCLI3829.1

Mamalakis, A., Yu, J. Y., Randerson, J. T., AghaKouchak, A., & Foufoula-Georgiou, E. (2018). A new interhemispheric teleconnection increases predictability of winter precipitation in southwestern US. *Nature Communications*, *9*(1), 1–10. https://doi.org/10.1038/s41467-018-04722-7

Minobe, S., Kuwano-Yoshida, A., Komori, N., Xie, S. P., & Small, R. J. (2008). Influence of the Gulf Stream on the troposphere. *Nature*, *452*(7184), 206–209. https://doi.org/10.1038/nature06690

Nogueira, R. C., & Keim, B. D. (2011). Contributions of Atlantic tropical cyclones to monthly and seasonal rainfall in the eastern United States 1960–2007. *Theoretical and Applied Climatology*, *103*(1–2), 213–227. https://doi.org/10.1007/s00704-010-0292-9

Pathak, R., Sahany, S., Mishra, S. K., & Dash, S. K. (2019). Precipitation biases in CMIP5 models over the South Asian egion. *Scientific Reports*, *9*(1), 1–13. https://doi.org/10.1038/s41598-019-45907-4

Roberts, M. J., Jackson, L. C., Roberts, C. D., Meccia, V., Docquier, D., Koenigk, T., et al. (2020). Sensitivity of the Atlantic meridional overturning circulation to model resolution in CMIP6 HighResMIP simulations and implications for future changes. *Journal of Advances in Modeling Earth Systems*, *12*(8), e2019MS002014. https://doi.org/10.1029/2019MS002014

Scaife, A. A., Arribas, A., Blockley, E., Brookshaw, A., Clark, R. T., Dunstone, N., et al. (2014). Skillful long-range prediction of European and North American winters. *Geophysical Research Letters*, *41*(7), 2514–2519. https://doi.org/10.1002/2014GL059637

Scaife, A. A., & Smith, D. (2018). A signal-to-noise paradox in climate science. *npj Climate and Atmospheric Science*, *1*(1), 28. https://doi.org/10.1038/s41612-018-0038-4

Schmidt, N., Lipp, E. K., Rose, J. B., & Luther, M. E. (2001). ENSO influences on seasonal rainfall and river discharge in Florida. *Journal of Climate*, *14*(4), 6152–6628. https://doi.org/10.1175/1520-0442(2001)014<0615:EIOSRA>2.0.CO;2

Schneider, U., Finger, P., Meyer-Christoffer, A., Rustemeier, E., Ziese, M., & Becker, A. (2017). Evaluating the hydrological cycle over land using the newly-corrected precipitation climatology from the Global Precipitation Climatology Centre (GPCC). *Atmosphere*, *8*(3), 52. https://doi.org/10.3390/atmos8030052

Seager, R., Tzanova, A., & Nakamura, J. (2009). Drought in the southeastern United States: Causes, variability over the last millennium, and the potential for future hydroclimate change. *Journal of Climate*, *22*(19), 5021–5045. https://doi.org/10.1175/2009JCLI2683.1

Shepherd, T. G. (2014). Atmospheric circulation as a source of uncertainty in climate change projections. *Nature Geoscience*, *7*(10), 703–708. https://doi.org/10.1038/ngeo2253

Siegert, S., Stephenson, D. B., Sansom, P. G., Scaife, A. A., Eade, R., & Arribas, A. (2016). A Bayesian framework for verification and recalibration of ensemble forecasts: How uncertain is NAO predictability? *Journal of Climate*, *29*(3), 995–1012. https://doi.org/10.1175/JCLI-D-15-0196.1

Siqueira, L., & Kirtman, B. P. (2016). Atlantic near-term climate variability and the role of a resolved Gulf Stream. *Geophysical Research Letters*, *43*(8), 3964–3972. https://doi.org/10.1002/2016GL068694

Siqueira, L., Kirtman, B. P., & Laurindo, L. C. (2021). Forecasting remote atmospheric responses to decadal Kuroshio stability transitions. *Journal of Climate*, *34*(1), 379–395. https://doi.org/10.1175/JCLI-D-20-0139.1

Small, R. D., deSzoeke, S. P., Xie, S. P., O'neill, L., Seo, H., Song, Q., et al. (2008). Air–sea interaction over ocean fronts and eddies. *Dynamics of Atmospheres and Oceans*, *45*(3–4), 274–319. https://doi.org/10.1016/j.dynatmoce.2008.01.001

Smith, D. M., Eade, R., Scaife, A. A., Caron, L. P., Danabasoglu, G., DelSole, T. M., et al. (2019). Robust skill of decadal climate predictions. *Npj Climate and Atmospheric Science*, *2*(1), 1–10. https://doi.org/10.1038/s41612-019-0071-y

Solomon, A., & Newman, M. (2012). Reconciling disparate twentieth-century Indo-Pacific ocean temperature trends in the instrumental record. *Nature Climate Change*, *2*(9), 691–699. https://doi.org/10.1038/nclimate1591

Strommen, K., & Palmer, T. N. (2019). Signal and noise in regime systems: A hypothesis on the predictability of the North Atlantic oscillation. *Quarterly Journal of the Royal Meteorological Society*, *145*(718), 147–163. https://doi.org/10.1002/qj.3414

Sugimoto, S., Qiu, B., & Schneider, N. (2021). Local atmospheric response to the Kuroshio large meander path in summer and its remote influence on the climate of Japan. *Journal of Climate*, *34*(9), 3571–3589. https://doi.org/10.1175/JCLI-D-20-0387.1

Trenberth, K. E., Branstator, G. W., Karoly, D., Kumar, A., Lau, N. C., & Ropelewski, C. (1998). Progress during TOGA in understanding and modeling global teleconnections associated with tropical sea surface temperatures. *Journal of Geophysical Research: Oceans*, *103*(C7), 14291–14324. https://doi.org/10.1029/97JC01444

Wang, H., Fu, R., Kumar, A., & Li, W. (2010). Intensification of summer rainfall variability in the southeastern United States during recent decades. *Journal of Hydrometeorology*, *11*(4), 1007–1018. https://doi.org/10.1175/2010JHM1229.1

Wang, S., Jing, Z., Zhang, Q., Chang, P., Chen, Z., Liu, H., & Wu, L. (2019). Ocean Eddy energetics in the spectral space as revealed by high-resolution general circulation models. *Journal of Physical Oceanography*, *49*(11), 2815–2827. https://doi.org/10.1175/JPO-D-19-0034.1

Williams, A., Cook, B. I., Smerdon, J. E., Bishop, D. A., Seager, R., & Mankin, J. S. (2017). The 2016 southeastern US drought: An extreme departure from centennial wetting and cooling. *Journal of Geophysical Research: Atmospheres*, *122*(20), 10–888. https://doi.org/10.1002/2017JD027523

Xu, H., Tokinaga, H., & Xie, S. P. (2010). Atmospheric effects of the Kuroshio large meander during 2004–05. *Journal of Climate*, *23*(17), 4704–4715. https://doi.org/10.1175/2010JCLI3267.1

Yoon, J. H., & Leung, L. R. (2015). Assessing the relative influence of surface soil moisture and ENSO SST on precipitation predictability over the contiguous United States. *Geophysical Research Letters*, *42*(12), 5005–5013. https://doi.org/10.1002/2015GL064139

Zhang, W. (2020). *Understanding decadal climate predictability in the global ocean*. (Doctoral dissertation). ProQuest Dissertations & Theses Global (order No. 28091098). University of Miami. Retrieved from http://access.library.miami.edu/login?url=https://www.proquest.com/dissertations-theses/understanding-decadal-climate-predictability/docview/2444730287/se-2?accountid=14585

Zhang, W., & Kirtman, B. (2019a). Estimates of decadal climate predictability from an interactive ensemble model. *Geophysical Research Letters*, *46*(6), 3387–3397. https://doi.org/10.1029/2018GL081307

Zhang, W., & Kirtman, B. (2019b). Understanding the signal-to-noise paradox with a simple Markov model. *Geophysical Research Letters*, *46*(22), 13308–13317. https://doi.org/10.1029/2019GL085159

Zhang, W., Kirtman, B., Siqueira, L., Clement, A., & Xia, J. (2021). Understanding the signal-to-noise paradox in decadal climate predictability from CMIP5 and an eddying global coupled model. *Climate Dynamics*, *56*, 2895–2913 https://doi.org/10.1007/s00382-020-05621-8